BIOLOGY OF REPRODUCTION (2016) **94**(2):39, 1–12
Published online before print 13 January 2016.
DOI 10.1095/biolreprod.115.135848

Maternal Smoke Exposure Impairs the Long-Term Fertility of Female Offspring in a Murine Model[1]

Nicole J. Camlin,[3,4] Alexander P. Sobinoff,[3,4,5] Jessie M. Sutherland,[4,6] Emma L. Beckett,[6] Andrew G. Jarnicki,[6] Rebecca L. Vanders,[6] Philip M. Hansbro,[6] Eileen A. McLaughlin,[2,4,7] and Janet E. Holt[6]

[4]*School of Environmental and Life Sciences, University of Newcastle, Callaghan, New South Wales, Australia*
[5]*Telomere Length Regulation Group, Children's Medical Research Institute, Westmead, New South Wales, Australia*
[6]*School of Biomedical Sciences & Pharmacy, University of Newcastle, Callaghan, New South Wales, Australia*
[7]*School of Biological Sciences, University of Auckland, Auckland, New Zealand*

ABSTRACT

The theory of fetal origins of adult disease was first proposed in 1989, and in the decades since, a wide range of other diseases from obesity to asthma have been found to originate in early development. Because mammalian oocyte development begins in fetal life it has been suggested that environmental and lifestyle factors of the mother could directly impact the fertility of subsequent generations. Cigarette smoke is a known ovotoxicant in active smokers, yet disturbingly 13% of Australian and 12% of US women continue to smoke throughout pregnancy. The focus of our investigation was to characterize the adverse effects of smoking on ovary and oocyte quality in female offspring exposed in utero. Pregnant mice were nasally exposed to cigarette smoke for 12 wk throughout pregnancy/lactation, and ovary and oocyte quality of the F1 (maternal smoke exposed) generation was examined. Neonatal ovaries displayed abnormal somatic cell proliferation and increased apoptosis, leading to a reduction in follicle numbers. Further investigation found that altered somatic cell proliferation and reduced follicle number continued into adulthood; however, apoptosis did not. This reduction in follicles resulted in decreased oocyte numbers, with these oocytes found to have elevated levels of oxidative stress, altered metaphase II spindle, and reduced sperm-egg interaction. These ovarian and oocyte changes ultimately lead to subfertility, with maternal smoke-exposed animals having smaller litters and also taking longer to conceive. In conclusion, our results demonstrate that in utero and lactational exposure to cigarette smoke can have long-lasting effects on the fertility of the next generation of females.

cigarette smoke, in utero, oocyte, ovary, subfertility

INTRODUCTION

In utero exposure to cigarette smoke has been linked to adverse health effects in offspring, including an increased risk of premature birth, fetal growth retardation, and morbidity, and in later life obesity, asthma and congenital heart defects [1–4]. This is of particular concern, because despite increased public awareness of the adverse effects of smoking during pregnancy, 11%–14% of women at reproductive age (20–45 y) in Australia smoke daily [5]. Furthermore ~13% of Australian women and ~12% of women in the United States continue to smoke throughout their pregnancy [6, 7]. Furthermore, a growing body of evidence suggests that gestational exposure to cigarette smoke negatively affects the fertility of female offspring, leading to early-onset menarche, reduced fecundability, and premature menopause [8–13]. A number of studies examining human ovaries have explored the potential mechanism underlying such altered fertility during early ovarian development (5–21 wk gestation); however, longer-term studies in humans have been limited [14–16].

Mammalian females are born with a finite number of germ cells that begin their development during fetal life [17]. At birth, these germ cells, known as ''oocytes,'' are meiotically arrested at prophase I within primordial follicles, with their number dictating the reproductive lifespan of an individual [18, 19]. These quiescent primordial follicles consist of an immature oocyte surrounded by a single layer of granulosa cells. As folliculogenesis continues the number of granulosa cell layers increases, with these somatic cells providing important factors, such as inhibin, to the developing oocyte [20]. Once fully matured, a surge of luteinizing hormone causes ovulation and releases the oocyte from its prophase I arrest [21]. It is important to note, however, that most follicles are destined to die, with only a select few reaching ovulation, making them a precious resource.

In vivo and in vitro exposure of human and mouse fetal ovaries to cigarette smoke or its constituents nicotine, DMBA-DHD, DMBA, or BaP has been found to negatively affect oocyte and follicle development by altering proliferation and apoptosis of germ and granulosa cells [14, 15, 19, 22–24], and modifying hormone production of estrogen, progesterone, and inhibin [14, 25]. In this study we used an animal model to examine the effects of in utero/lactational exposure to whole

[1]Supported by Australian Research Council, National Health and Medical Research Council grant NHMRC 510735 to E.A.M. and P.M.H.; Hunter Medical Research Institute, Newcastle Permanent Building Society Charitable Trust grant HMRI 06-34; and the University of Newcastle Priory Research Centre in Chemical Biology. P.M.H. was supported by an NHMRC Principal Research Fellowship. J.E.H. was supported by an Australian Research Council DECRA award (DE120101242). N.J.C., A.P.S., and J.M.S. were supported by Australian Post Graduate Awards. Presented in part at the 44th annual meeting for the Society of Reproductive Biology, August 25–28, 2013, Sydney, Australia; the 45th annual meeting for the Society of Reproductive Biology, August 24–27, 2014, Melbourne, Australia; and the EMBO Conference on Meiosis, August 30–September 4, 2015, Oxford, England.
[2]Correspondence: Eileen A. McLaughlin, PRC in Chemical Biology, School of Environmental & Life Sciences, University of Newcastle, Callaghan, NSW 2308, Australia.
E-mail: eileen.mclaughlin@newcastle.edu.au
[3]These authors contributed equally to this work.

Received: 28 September 2015.
First decision: 21 October 2015.
Accepted: 5 January 2016.

eISSN: 1529-7268 http://www.biolreprod.org
ISSN: 0006-3363

cigarette smoke on female fertility using our novel nose-only inhalation model [26–31]. Exposure of mice to cigarette smoke via this nose-only inhalation model for 8 wk leads to smoke-induced chronic obstructive pulmonary disease, which is evident in humans after years of cigarette smoking [26]. Our investigation focuses on both the short-term and long-term consequences of maternal cigarette exposure (MSE) on an offspring's ovarian and oocyte quality, and ultimately their fertility.

MATERIALS AND METHODS

All reagents were obtained from Sigma-Aldrich (St. Louis, MO) unless otherwise specified.

Animals and Ethics Approval

All experiments were performed with the approval of the University of Newcastle Animal Care and Ethics Committee. C57BL/6 mice were obtained from Australian BioResources and housed with ad libitum food and water under a 12L:12D lighting regimen.

Smoke Exposure

Six-week-old female mice were exposed to smoke as previously described [26, 29, 31]. Briefly animals were nasally exposed to mainstream cigarette smoke (twelve 3R4F reference cigarettes; University of Kentucky) for 75 min twice daily, 5 days a week for 12–13 wk, in individual mouse chambers, preventing passive smoking of breeding males and pups. On Week 5 females were housed with non-cigarette smoke-exposed males (two females per male) until visibly pregnant (abdominal bulge observable from approximately Gestational Day 14). Smoke exposure continued throughout pregnancy and lactation, ceasing once pups (F1 generation) were weaned on Postnatal Days 21–23 (PNDs 21–23) [28].

Fertility Trial

Four F1 females (age 6 wk) per treatment group were housed with non-cigarette smoke-exposed males (age 8 wk) continuously. Date of birth and size of litters were recorded during a 3-mo period. Conception date was determined by subtracting 19 days from time of litter drop.

Follicle Counts and Staging

Three Bouin-fixed PND 6, 8- to 9-wk-old, and 9-mo-old ovaries per group were paraffin embedded and sectioned at 5 μm prior to hematoxylin and eosin staining. The PND 6 follicle counts were performed on every fifth section for half the ovary. The 8- to 9-wk-old and the 9-mo-old follicle counts were performed on every 15th section for the entire ovary. Only follicles with a visible oocyte nucleus were counted. The PND 6 follicles were staged through oocyte size. Oocyte diameters were measured using ImageJ software (freeware; National Institutes of Health); those with a diameter of $<$15 μm were classed as primordial, 15–20 μm as activated follicles, and $>$20 μm as primary follicles. Morphological features were used to stage follicles in adult ovaries. Briefly, primordial follicles have a single layer of squamous pregranulosa cells surrounding the oocyte. Primary follicles are characterized by a single layer of cuboidal granulosa cells. By secondary stage, a zona pellucida (ZP) has formed around the growing oocyte, which is surrounded by multiple layers of granulosa cells with a theca externa. Finally, a follicle fluid-filled antral cavity forms in antral follicles [19].

Immunofluorescence

Three Bouin-fixed PND 3, PND 6, 8- to 9-wk-old, and 9-mo-old ovaries per treatment were deparaffinized and rehydrated before antigen retrieval in Tris buffer (50 mM, pH 10.6). Sections were blocked in 3% bovine serum albumin (BSA) before incubation with primary antibodies active caspase 3 (1:200; ab13847; Abcam) for 1 h at room temperature or proliferating cell nuclear antigen (PCNA; 1:100; NA03; Merick Millipore) and AMH (1:20; MCA2246; AdB Serotec) overnight at 4°C. The appropriate secondary antibody conjugated to Alexa 594 (1:200; Life Technologies) was applied for 1 h at room temperature. Slides were again washed and counterstained with DAPI before mounting in citifluor (Citifluor Ltd.). An Axio Imager A1 epifluorescent microscope (Carl Zeiss MicroImaging Inc.) was used to visualize sections, with photomicrographs taken using an Olympus DP70 microscope camera (Olympus America). Fluorescence intensity analysis was performed using ImageJ on ovaries from at least three animals, across three replicates, as previously described by McCloy et al. [32].

TUNEL Analysis

Sections were treated with 20 μg/ml proteinase K (Promega) prior to TUNEL analysis using ApopTag Fluorescein In Situ Apoptosis Detection Kit (S7110; Merick Millipore) according to the manufacturer's protocol. DAPI was used to counterstain sections before mounting in citifluor (Citifluor) and imaging on an Axio Imager A1 epifluorescent microscope with an Olympus DP70 microscope camera. Total cells and TUNEL-positive cells were counted using ImageJ and used to calculate the proportion of TUNEL-positive cells.

Metaphase II Egg Collection and Fixation

Female mice were intraperitoneally injected with 7.5 IU of pregnant mares' gonadotropin (Intervet), followed by 5 IU of human chorionic gonadotropin (Intervet) 48 h later. Metaphase II arrested (MII) eggs were collected 12 h later from the ampulla into M2 media with BSA containing hyaluronidase (H4272) to remove cumulus cells. Oocytes were washed into M2 containing monastrol (200 μM; M8515) for 2 h to collapse the spindle for aneuploidy analysis or were fixed with 4% paraformaldehyde in PBS with 0.5% Triton X-100 for 30 min [33]. Following monastrol treatment, oocytes were fixed as described above.

Germinal Vesicle Oocyte Collection and In Vitro Maturation

Ovaries were dissected from 9-mo-old females, with one ovary per animal used for germinal vesicle (GV) oocyte collection. Briefly, preantral follicles were punctured with a 33.5-gauge needle, releasing cumulus-oocyte complexes into M2 with BSA and milrinone (M4659). Oocytes were denuded of cumulus cells, washed into MEM media (11900-024; Life Technologies), and allowed to undergo in vitro maturation in 5% CO_2 at 37°C. After 16 h oocytes were scored for the presences of a polar body (MII oocytes), with MII oocytes treated with monastrol and fixed as described above.

Oocyte Oxidative Stress Determination

Oocyte lipid peroxidation and mitochondrial superoxide leakage were analyzed as previously described by Sobinoff et al. [27] on oocytes from three animals per treatment. Briefly, MII eggs were collected from 8-wk-old F1 females and incubated in either 10 mM 4,4-difluoro-5-(4-phenyl-1,3-butta-dienyl)-4-bora-3a,4a-diaza-s-indacene-3-undecanoic acid 581/591 C11 (BODIPY; D-2228; Life Technologies) or 5 μM MitoSOX red stain (M36008; Life Technologies) for 20 or 30 min, respectively. Positive control eggs were obtained by treatment with 5 μM menadione (MEN) prior to BODIPY or MitoSOX red exposure. Eggs were washed into M2, mounted, and imaged with an LSM510 laser-scanning microscope (Carl Zeiss). Lipid peroxidation was determined by the shift in BODIPY fluorescence from red to green (red:green ratio). Superoxide leakage was indicated by increasing MitoSOX red fluorescence.

Oocyte Immunocytochemistry

Immunocytochemistry was performed on oocytes from three to four animals per treatment using anti-α-tubulin (1:400; A11126; Life Technologies) or anti-CREST (1:400; 90C-CS1058; Bioclone Australia) overnight at 4°C after blocking in 7% goat serum/PBS-0.1% Tween-20. Oocytes were washed through 1% BSA in PBS-0.1% Tween-20 prior to incubation with secondary antibodies conjugated with Alexa 555 or Alexa 633 (1:1000; Life Technologies). Oocytes were counterstained in Hoechst (20 μg/ml) and mounted in citifluor. Imaging was performed on an Olympus FV1000 using a 60×/1.2 N.A. UPLSAPO oil immersion objective lens (Olympus). ImageJ was used to measure spindle size and count kinetochores using a macro designed by Dr. Simon I.R. Lane [34]. For ZP analyses, four measurements were taken from the transmission image of each egg to calculate mean thickness (Supplemental Fig. S1; Supplemental Data are available online at www.biolreprod.org), as previously described by Jennings et al. [35].

Sperm-Egg Binding Assays

Freshly collected MII eggs were examined for sperm-zona and sperm-oolemma binding as previously described by Sobinoff et al. [27] on three

animals per treatment. Briefly, MII oocytes were collected in M2 media with hyaluronidase to remove cumulus cells. For sperm-oolemma binding assays, the zona was removed from eggs using Acid Tyrode solution (T1788). Sperm was collected from the cauda epididymides of a mature untreated male mice and morphology analyzed. Morphologically normal samples were allowed to capacitate for 3 h at 37°C. Eggs with or without their ZP were incubated with capacitated sperm at 2×10^5 sperm per milliliter in M2 medium for 15 min before being washed into sperm-free media. Phase microscopy was used to count sperm heads bound to the zona or oolemma.

Statistics

Statistical analysis was performed using GraphPad Prism 6.0 software (GraphPad Software Inc.). For categorical data, Fisher exact test was used. All other data were tested from normal distribution using D'Agnostino-Pearson omnibus normality test. For data found to follow a normal distribution, Student *t*-test or ANOVA with Tukey post hoc was used. For all other data, Mann-Whitney test or Kruskal-Wallis test with Dunn post hoc statistical test was performed. A P value <0.05 was considered statistically significant. Further information on statistics tests used for each data set can be found within the figure legends.

RESULTS

Maternal Smoke Exposure Alters Neonatal Follicle Population

Initially we investigated the neonatal ovarian consequences for female mice whose ovaries had been exposed to the products of inhaled cigarette smoke in utero (maternally smoke exposed, herein referred to as ''MSE mice''). PND 6 ovaries that normally possess only primordial and newly activated primary follicles were examined. Strikingly, MSE ovaries only contained around half the number of follicles compared with controls (305 ± 63 [MSE] vs. 595 ± 173 [control], $P = 0.0079$; Fig. 1A). Classification of follicles based on size found MSE ovaries contained a higher proportion of primordial follicles (<15 μm; 46.6% ± 5.5% vs. 31.7% ± 4.5%, $P = 0.0222$; Fig. 1B), but activating (15–20 μm) and primary (>20 μm) follicle populations were unchanged (36.5% ± 3.4% vs. 40.4% ± 1.3% and 16.8% ± 5.6% vs. 27.9% ± 4.4%, respectively; Fig. 1B).

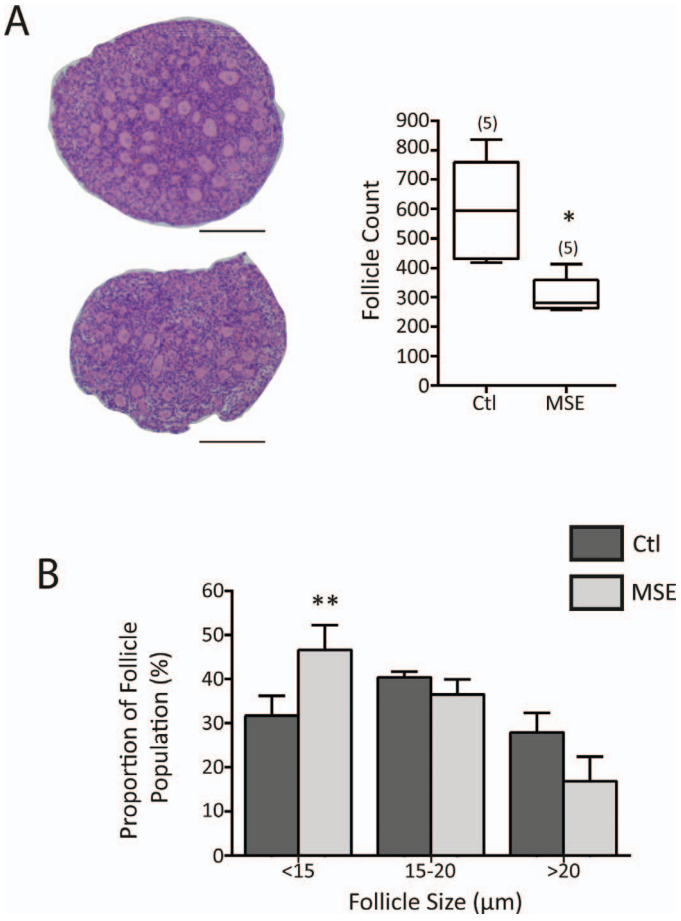

FIG. 1. Maternal smoke exposure alters the neonatal follicle pool. **A**) Average number of follicles per PND 6 ovary (half); *$P = 0.0079$; Mann-Whitney test; bar = 50 μm; ×100 magnification used; n = 5. Box outline, 25th to 75th percentiles; centerline, median; whiskers, 10th to 90th percentiles. **B**) Classification of follicles based on size revealed that PND 6 MSE ovaries had an increased number of primordial follicles (<15 μm; **$P = 0.0222$, Student *t*-test), with no change in activating or primary follicles observed; n = 3. Values are shown as mean with SD marked.

MSE Neonatal Ovaries Display Abnormal Levels of Cellular Apoptosis and Proliferation

To elucidate the mechanisms behind the altered follicle population observed at PND 6, examination of neonatal ovaries for markers of apoptosis revealed that DNA fragmentation as examined by TUNEL assay was significantly elevated in MSE ovaries at PNDs 3 and 6 (positive cells, respectively: PND 3, 12.7% ± 8.6 vs. 1.0% ± 0.2%, $P = 0.0090$; and PND 6, 7.4% ± 3.5% vs. 1.3% ± 1.7%, $P = 0.0013$; Fig. 2A). To confirm this, a second marker of apoptosis, active caspase 3, was examined and was also found to be elevated in both the oocytes and granulosa cells of MSE females at PNDs 3 and 6 (~8-fold and ~52-fold, $P = 0.0088$ and $P = 0.0007$, respectively; Fig. 2B).

To determine whether proliferation of ovarian somatic cells, including granulosa cells, was affected by MSE, we analyzed PCNA expression, which has previously been correlated with the initiation of follicle growth [36]. Immunosignal, found primarily in ovarian somatic cells, was decreased in MSE ovaries at PND 3 (~0.5-fold, $P = 0.0102$; Fig. 2C); however, by PND 6, the signal was significantly increased relative to controls (~1.5-fold, $P = 0.0194$; Fig. 2C).

MSE Alters Adult Ovary Size and Follicle Population

To determine whether ovarian alterations persisted into adulthood, when animals were no longer lactationally exposed to cigarette smoke, ovaries from 8- to 9-wk-old (virgin) and 9-mo-old (nonvirgin) control and MSE females were examined. Ovarian weights of MSE females were found to be significantly lower than controls when normalized to body weight at 8–9 wk but not 9 mo ($2.0 \times 10^{-4} \pm 2.8 \times 10^{-5}$ vs. $4.5 \times 10^{-4} \pm 1.5 \times 10^{-4}$, and $2.7 \times 10^{-4} \pm 6.8 \times 10^{-5}$ vs. $2.4 \times 10^{-4} \pm 3.36 \times 10^{-5}$ ovary:body weight ratio respectively, $P = 0.0189$; Fig. 3, A and C). Furthermore, the reduction in follicle numbers seen at PND 6 did not persist at 8–9 wk, with MSE ovaries containing equivalent follicle numbers compared with controls (39.3 ± 16.3 vs. 47.3 ± 12.0; Fig. 3B). Additionally, there was no change in the proportions of different follicle stages or corpus luteum (Fig. 3B). By 9 mo, however, there was once again a significant decrease in follicle numbers in MSE ovaries compared with controls (34.0 ± 19.4 vs. 80.3 ± 14.7, $P = 0.0089$; Fig. 3D).

MSE Adult Ovaries Display Abnormal Levels of Cellular Proliferation but No Apoptosis

To determine if changes in ovarian somatic cell proliferation continued into adulthood, 8- to 9-wk-old and 9-mo-old ovaries were examined for PCNA expression that localized primarily to granulosa cells in secondary and antral follicles. At 8–9 wk,

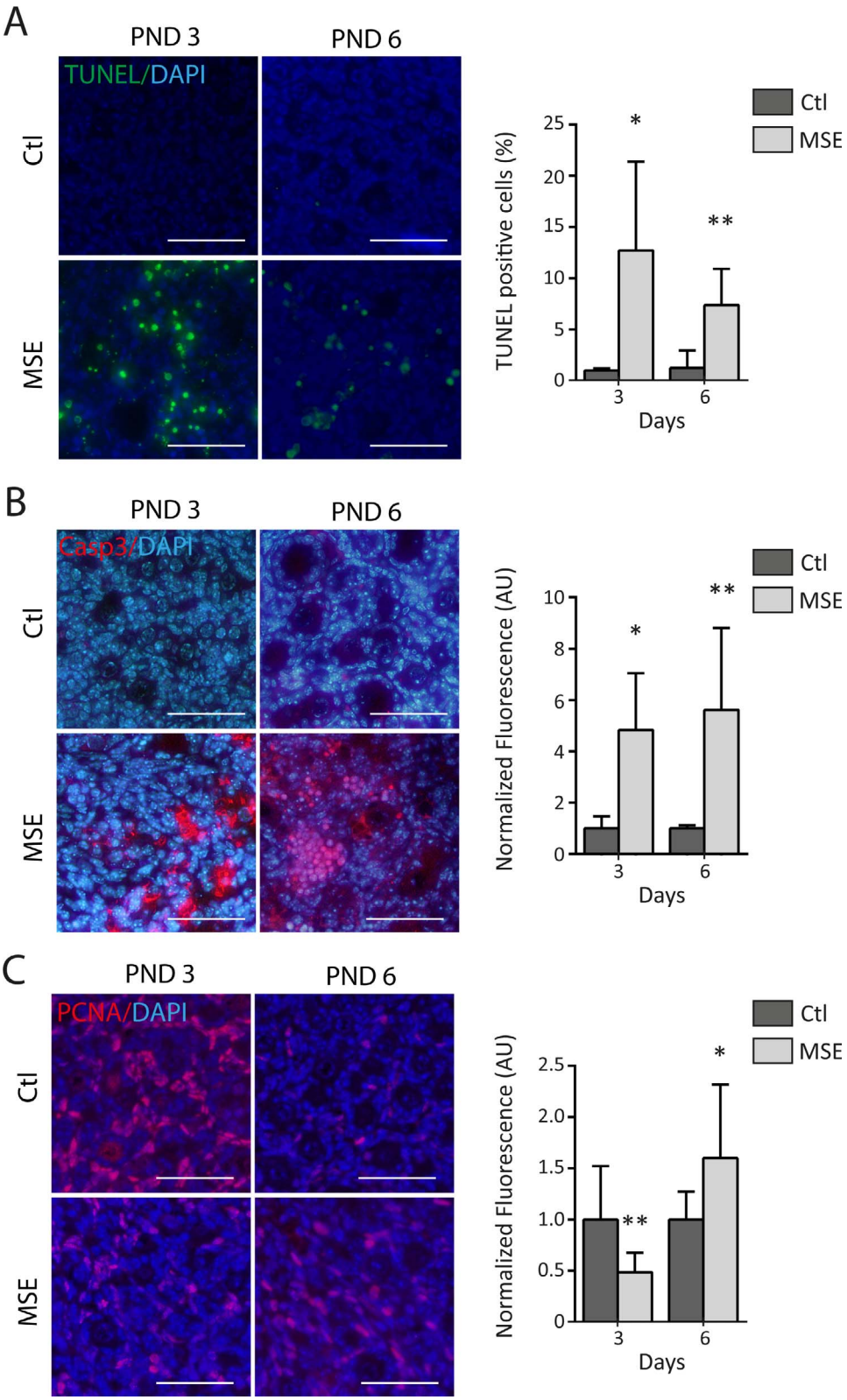

FIG. 2. Maternal smoke exposure increases neonatal ovarian apoptosis and alters proliferation. **A**) TUNEL staining (green) of neonatal control and MSE ovaries at ×200 magnification. Graphical representation of the number of TUNEL-positive cells in controls versus MSE at PND 3 (*$P = 0.0090$) and PND 6 (**$P = 0.0013$, Mann-Whitney test). **B**) Fluorescent immunolocalization of activated caspase 3 (red) at ×200 magnification. Graphical representation of average ovarian fluorescence per section in control versus MSE at PND 3 (*$P = 0.0088$) and PND 6 (**$P = 0.0007$, Mann-Whitney test). **C**) Fluorescent immunolocalization of cellular proliferation marker PCNA (red) at ×200 magnification. Graphical representation of average ovarian fluorescence per section in control versus MSE at PND 3 (**$P = 0.0102$) and PND 6 (*$P = 0.0194$, Student *t*-test). Nuclei of all sections counterstained with DAPI (blue). Sections analyzed from three control/smoked animals per age group. Values are shown as mean with SD marked. Bar = 50 μm.

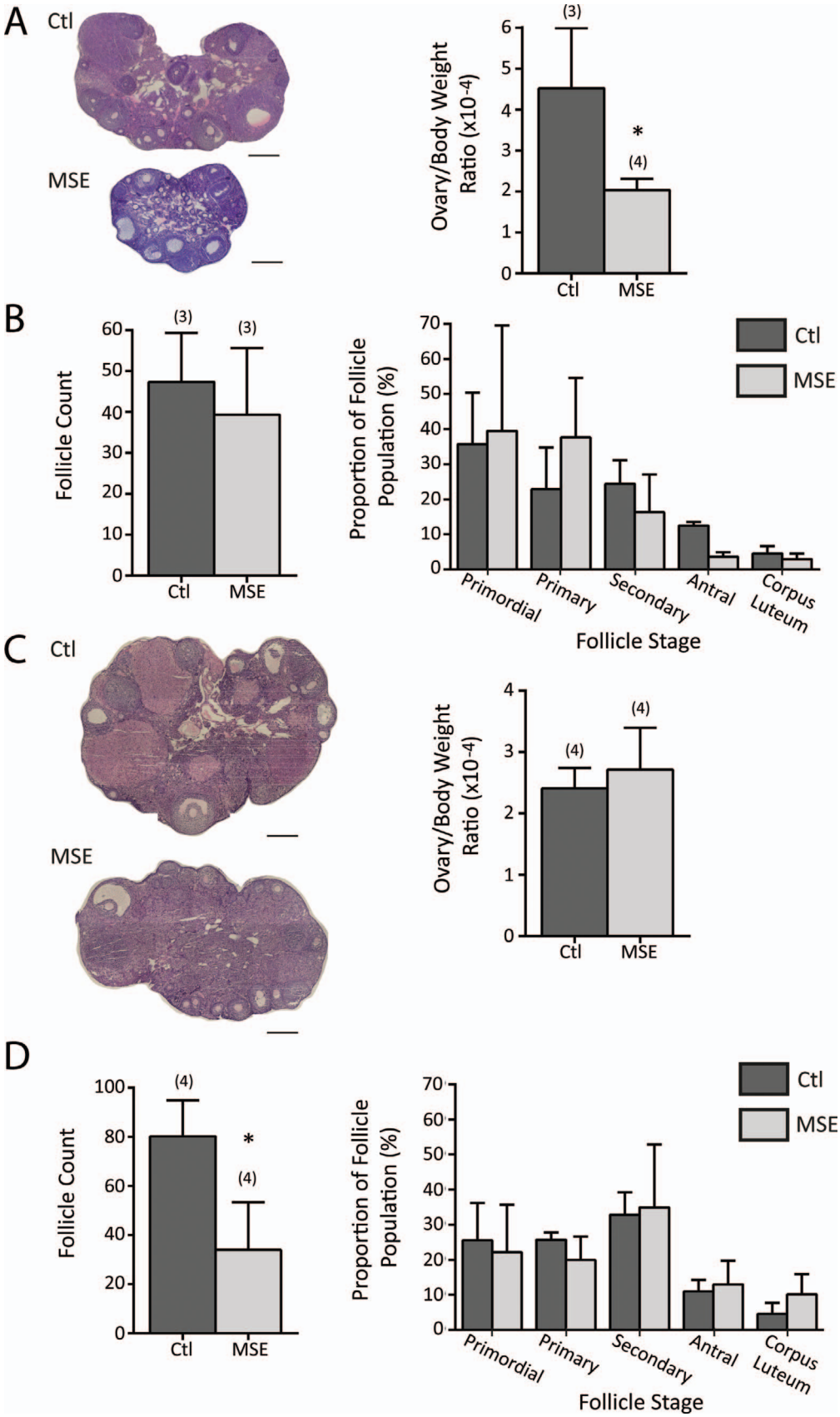

FIG. 3. Maternal smoke exposure alters adult ovarian size and follicle population. **A**) Representative image of control and MSE ovaries at 8–9 wk. Graphical representation of average ovary size at 8 wk normalized to body weight (*$P = 0.0189$, Student *t*-test). **B**) Average number of follicles per ovary at 8–9 wk ($P = 0.5307$, Student *t*-test). Classification of follicles based on morphology revealed no change in follicle or corpora lutea population. **C**) Representative image of control and MSE ovaries at 9 mo, magnification ×100. Graphical representation of the average ovary size at 9 mo normalized to body weight ($P = 0.4505$, Student *t*-test). **D**) Average number of follicles per ovary at 9 mo (*$P = 0.0089$, Student *t*-test). Classification of follicles based on

MSE ovaries again had greatly decreased PCNA levels, presumably due to the lower numbers of proliferating follicles present, because PCNA at this age is most often associated with replicating granulosa cells of large preantral and antral follicles (~10-fold, $P < 0.0001$; Fig. 4A). Interestingly, however, by 9 mo MSE displayed an increase in PCNA fluorescence compared with controls (~2-fold, $P = 0.0011$; Fig. 4A). To investigate the possible cause of this elevated PCNA proliferation at 9 mo, ovaries were examined for AMH because it has been shown to reduce follicle proliferation [37]. Immunosignal of AMH that localized to granulosa cells in secondary and early antral follicles was significantly reduced in MSE ovaries (~2-fold, $P = 0.0013$; Fig. 4B). Further examination of ovaries for markers of apoptosis found no change in TUNEL-positive cells at 8–9 wk or 9 mo (Fig. 4C).

Reduced Oocyte Number and Quality in MSE Animals

Having established a reduction in preantral follicle number, as well as altered somatic cell proliferation and survival, in the ovaries of MSE females, we next assessed the number and quality of mature eggs isolated from these mice after hormonal stimulation. As expected, MSE females ovulated fewer MII eggs compared with controls at 8 wk (21 ± 2.8 vs. 28 ± 2.4, $P = 0.0001$; Fig. 5A). Furthermore, at 9 mo a reduced number of mature GV oocytes were collected from MSE ovaries (8.0 ± 0.8 vs. 13.2 ± 2.6, $P = 0.0088$; Fig. 5B). To determine the oxidative stress status of 8-wk-old eggs, we examined lipid peroxidation and mitochondrial superoxide leakage using the cell-permeable probes BODIPY and MitoSOX red, respectively. Superoxide leakage was increased approximately ~2-fold in MSE eggs ($P = 0.0113$; Fig. 5C), as was lipid peroxidation, which was 1.5-fold higher ($P < 0.0001$; Fig. 5D). Oxidative stress has been hypothesized to lead to poor oocyte quality, including increased incidence of aneuploidy [38]. Interestingly, however, there was no change in the aneuploidy rate between MSE and control animals at 4 wk or 9 mo of age (Supplemental Fig. S2), indicating normal chromosome segregation was likely to have taken place during meiosis I in these eggs.

Aneuploidy can also arise during completion of meiosis II, so we next examined the shape and size of the MII spindle, which can provide an indication of whether this second meiotic division is likely to occur normally. Both spindle pole-to-pole length (13.9 ± 1.2 vs. 15.1 ± 1.3 μm, $P < 0.0001$; Fig. 6) and spindle width (8.9 ± 1.0 vs. 10.7 ± 1.1 μm, $P < 0.0001$; Fig. 6) were smaller in MSE oocytes compared with controls, which suggests that completion of meiosis II after fertilization could be compromised.

Decreased Sperm-Egg Interaction with MSE

The interaction of eggs from MSE ovaries with wild-type sperm was also investigated to determine the likelihood of normal conception. The MSE animals had a reduction in both sperm-zona binding (14 ± 3.5 vs. 23 ± 5.2 bound sperm per egg, $P = 0.0007$; Fig. 7A) and sperm-oolemma binding (17 ± 4.6 vs. 24 ± 3.5 bound sperm per egg, $P < 0.0001$; Fig. 7B) compared with controls. We also observed that ZP thickness was reduced in MSE animals at 4 wk (5.7 ± 0.6 vs. 7.0 ± 0.8 μm, $P < 0.0001$; Fig. 7C). By 9 mo there was no difference between control and MSE ZP thickness (7.8 ± 0.6 vs. 7.9 ± 0.6 μm); however, ZPs of both groups were significantly thicker compared with 4-wk animals ($P < 0.0001$; Fig. 7C). Together these results suggest that maternal smoke exposure leads to reduced quality of the egg plasma membrane and glycoprotein extracellular matrix, which may impact the success of fertilization.

MSE Decreases F1 Female Fertility

Finally, we sought to establish the overall reproductive consequences for MSE females. Control and MSE female adult mice (age 6 wk) were mated with non-smoke-exposed males during a period of 3 mo, and the days to conception, litter sizes, and pup weights were recorded. Time to conception was significantly increased in MSE females (8.2 ± 7.7 vs. 3.3 ± 2.5 days, $P = 0.0206$; Fig. 8). Additionally, a small but significant reduction in litter size was also found in MSE mice compared with controls (6 ± 1.6 vs. 7 ± 1.8 pups per litter, $P = 0.0190$; Fig. 8) with no significant change in pup weights, suggesting phenotypically normal litters (Supplemental Fig. S3).

DISCUSSION

In utero exposure to cigarette smoke in humans has been linked to adverse health effects in offspring, including increased risk of obesity, asthma, and congenital heart defects, and reduced female reproductive capacity [1–3, 8–13]. Through the use of our novel animal model we have been able to avoid external confounding factors present in human epidemiological studies of smoking and have begun to unravel the effects of maternal smoke exposure directly on the fertility of the subsequent generation of females. In the current study, we have identified ovarian and oocyte changes associated with pregnancy and lactational smoke exposure in the mouse that may underlie the reduced fecundability and early-onset menopause observed following human maternal exposure. Interestingly, changes in oocyte and ovarian quality observed in MSE mice are similar to alterations detected in their mothers [27].

Smoke exposure during the gestational/weaning period resulted in the loss of nearly half the ovarian follicle population at PND 6. In the mouse, the entire cohort of primordial follicles, from which all mature oocytes are ultimately derived, is established during early postnatal life, with some follicles beginning to enter the growing pool. Therefore, the time after birth is crucial in determining the reproductive capacity of the adult female. At PNDs 3–6 we observed increased levels of TUNEL, which suggests that loss of primordial and/or activated follicles is occurring at this time through an apoptosis-mediated mechanism. Such a mechanism of germ cell depletion has been observed in in vitro studies where neonatal ovaries were exposed to individual chemical constituents of cigarette smoke. For example, culture of PND 3–4 ovaries in the presence of benzo[a]pyrene, 3-methylcholanthrene, or 7,12-dimethylbenz[a] anthracene resulted in increased follicle apoptosis with an elevation in activated caspase 2, caspase 3, and DNA strand breaks (TUNEL) [39–41]. It is possible that germ cell apoptosis in MSE females may be initiated prior to birth, in the developing fetal ovary when early meiotic events are taking place. This could contribute to the

morphology revealed that despite a decrease in total follicle number, there was no change to the proportion of follicle types or corpora lutea. Values are shown as mean with SD marked. Bar = 300 μm, magnification ×100.

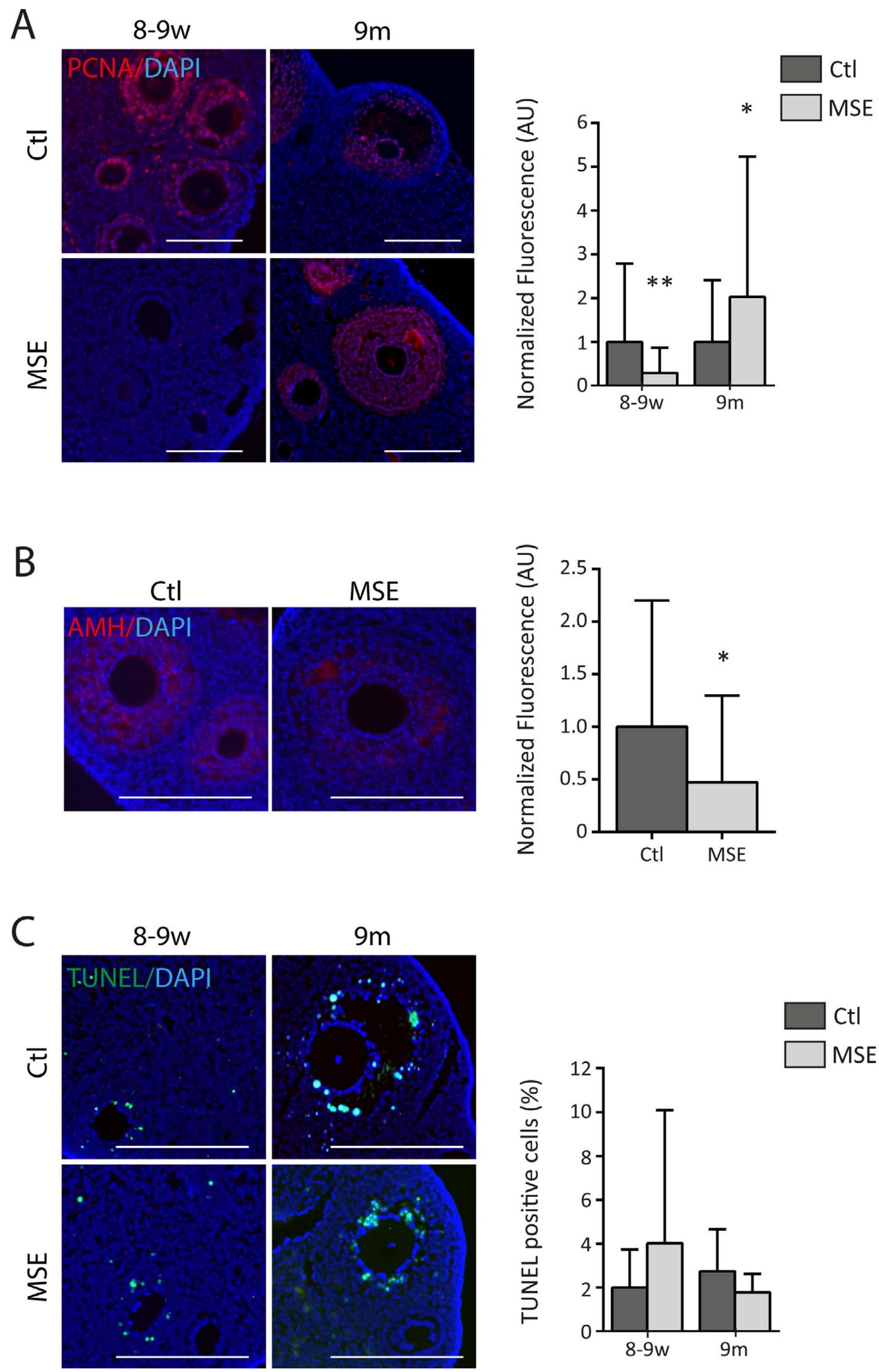

FIG. 4. Maternal smoke exposure altered adult ovarian cell proliferation. **A**) Fluorescent immunolocalization of cellular proliferation marker PCNA (red) at ×100 magnification. Graphical representation of average ovarian fluorescence per section in control versus MSE at 8–9 wk (**$P < 0.0001$, Mann-Whitney test) and 9 mo (*$P = 0.0011$, Mann-Whitney test). **B**) Fluorescent immunolocalization of AMH (red) at ×200 magnification. Graphical representation of average ovarian fluorescence per section in control versus MSE at 9 mo (*$P = 0.0013$, Mann-Whitney test). **C**) TUNEL staining (green) of adult control and MSE ovaries at ×200 magnification. Graphical representation of the number of TUNEL-positive cells in controls versus MSE at 8–9 wk ($P = 0.9817$, Mann-Whitney test) and 9 mo ($P = 0.1384$, Student *t*-test). Nuclei of all sections counterstained with DAPI (blue). Sections analyzed from three control/smoked animals per age group. Values are shown as mean with SD marked. Bar = 200 μm.

reduction in follicle numbers observed in neonatal MSE ovaries. In support of this concept, the culture of mouse fetal ovaries with polycyclic aromatic hydrocarbons or in utero exposure of human fetuses to cigarette smoke has been shown to significantly elevate proapoptotic markers Bax and HRK [14, 24]. In addition, data from our male MSE model indicate

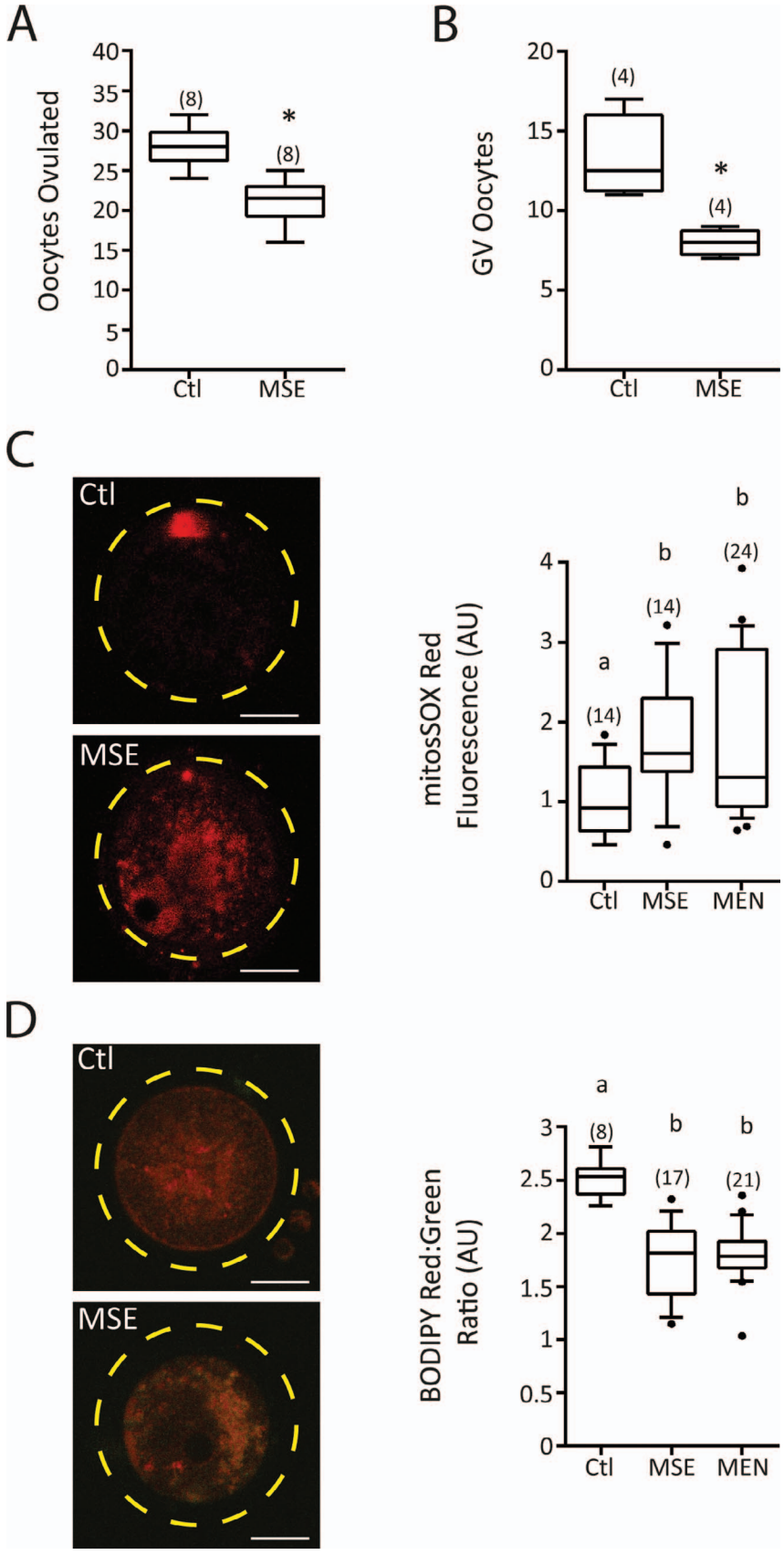

FIG. 5. Maternal smoke exposure reduces oocyte number and increases oocyte oxidative stress. **A**) Average number of oocytes ovulated per female at 8 wk (n = 8 control/MSE animals, *$P = 0.0001$, Student *t*-test). **B**) Average number of immature GV oocytes collected from one ovary per female at 9 mo (n = 4 control/MSE animals, *$P = 0.0088$, Student *t*-test). **C**) Representative image of MII oocyte at 8 wk probed with MitoSOX Red at ×600 magnification. n, number of oocytes examined from three control/MSE animals, $P = 0.0113$, Kruskal-Wallis test with Dunn post hoc test. **D**) Representative image of MII oocytes at 8 wk probed with BODIPY at ×600 magnification. n, number of oocytes examined from three control/MSE animals, $P < 0.0001$, Kruskal-Wallis

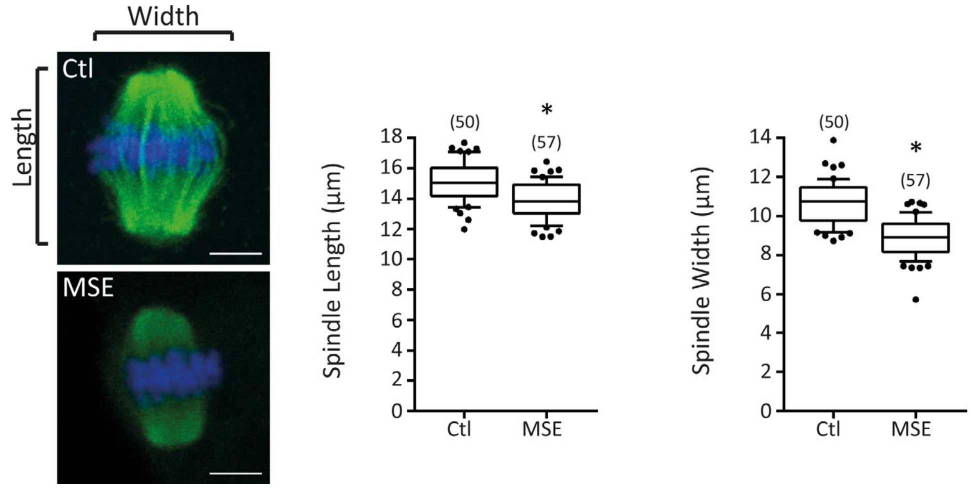

FIG. 6. Maternal cigarette smoke exposure decreases the metaphase II spindle size in ovulated oocytes. Representative confocal images of control and MSE oocytes immunostained for α-tubulin (green) at 600x magnification. Chromosomes are counterstained with Hoechst (blue). Graphical representations of median MII spindle length/width (centerline); box outline 25th–75th percentiles and whiskers, 10th–90th percentiles. n, number of oocytes examined from three control/MSE animals. *$P < 0.0001$, Student *t*-test, Bar = 5μm.

that meiotic spermatocytes are particularly susceptible to apoptosis following smoke exposure [28]. Future investigations examining the female MSE model at embryonic stages may assist in our understanding of how smoke exposure impacts early female meiosis.

Together with increased apoptosis in the neonatal ovary, we noted reduced proliferation of ovarian somatic cells at PND 3. Elevations in granulosa PCNA have previously been correlated with the initiation of follicle growth [36]. This reduced PCNA expression at PND 3, in conjunction with the increased proportion of primordial follicles at PND 6, indicated that in MSE ovaries, primordial follicles are failing to activate and transition to the growing pool in a timely manner. Interestingly, PCNA expression in both stromal and granulosa cells was elevated in MSE ovaries by PND 6. In addition to being a marker of S-phase, PCNA is involved in DNA repair [42], and so the elevation observed in MSE neonatal ovaries may reflect increased DNA repair activity. Our previous work in MSE males also revealed an increase in PCNA and DNA repair protein DCM1 in testis, indicating that gestational/neonatal exposure to cigarette smoke can lead to significant DNA damage and subsequent activation of repair and/or apoptotic pathways [28]. PCNA signal in control 8- to 9-wk ovaries was detected as expected, with numerous immunopositive granulosa cells present in preantral and antral follicles. We predict that the severe reduction in PCNA levels in adult MSE ovaries reflects abnormal granulosa cell proliferation, and therefore abnormal follicle growth. Despite this decreased PCNA expression, only a slight, nonsignificant reduction in the follicle population was observed at 8–9 wk. Because the ovarian follicle pool is established in neonatal life, it is therefore possible that this normalization in the follicle pool is a result of delayed follicle activation. During follicle activation and maturation the vast majority of follicles undergo atresia [43, 44]. The delay in follicle activation observed in PND 6 ovaries could result in the apparent follicular population catch-up in MSE ovaries at 8–9 wk; however, by late adult life (9 mo) follicle numbers were significantly reduced. Follicle-stimulating hormone (FSH) has been shown to increase PCNA expression in granulosa cells, and it is therefore possible that despite the apparently normal histological follicle population, the MSE ovaries are less sensitive to hormonal cues, resulting in the reduction of ovulated eggs observed [45, 46]. By 9 mo of age MSE ovaries contained significantly fewer follicles, resulting in a reduction of mature GV oocytes. Interestingly, however, PCNA expression was increased in MSE ovaries. We hypothesize that the elevation in follicular proliferation observed was the result of altered hormone dynamics within the ovary. One hormone in particular, AMH, which reduces follicular sensitivity to FSH and subsequently prevents follicle growth, is known to decrease in women near the end of their reproductive life [37, 47, 48]. In contrast to this, FSH levels are found to increase in these women [48]. Our investigation of AMH levels in reproductively aged females (9 mo) revealed decreased AMH levels in MSE ovaries. It is therefore possible that MSE animals are displaying a more severe aging phenotype than controls. Reduced AMH levels may be leading to elevated granulosa proliferation as a result of increased sensitivity to raised FSH levels.

It is important to note, however, that a previous study indicated that smoke-exposed F0 females are significantly smaller than controls [26]. Several human studies have found altered serum cholesterol levels in women with premature ovarian failure [49, 50]. Cholesterol is an essential precursor for estrogen and is therefore important for normal fetal ovarian development [51]. As such, it is possible that the reduction in the ovarian reserve of MSE animals could be the result of exposure to ovotoxic cigarette smoke constituents in combination with reduced maternal body mass.

In addition to the loss of both immature and mature oocyte numbers, gestational/neonatal exposure to cigarette smoke also reduced mature oocyte quality, with respect to oxidative stress status. The key source of oxidative stress in MSE oocytes may well be endogenous from damaged mitochondria, which

test with Dunn post hoc test. Bar = 20 μm. Box plot shows mean (centerline) with box outline 25th–75th percentiles and whiskers 10th–90th percentiles. **C** and **D**) MEN used as positive control.

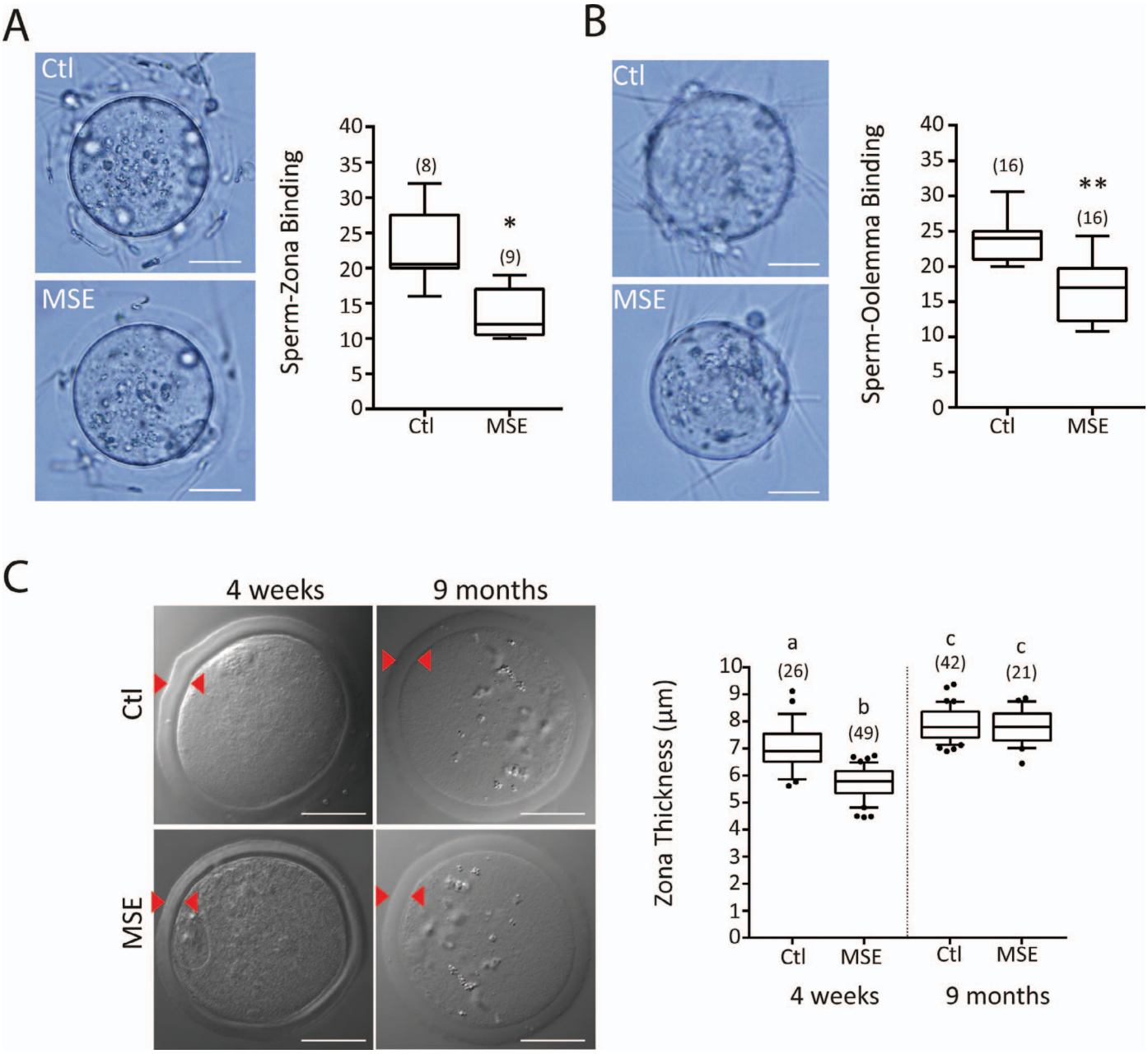

FIG. 7. Maternal smoke exposure alters sperm-egg interaction and ZP thickness. **A**) Representative images of sperm bound to the ZP of 8-wk MII oocytes at ×600 magnification. Graphical representation shows median number of sperm bound. n, number of oocytes examined from three control/MSE animals, $^{*}P = 0.0007$, Student *t*-test. **B**) Representative images of sperm bound to the oolemma of zona-free 8-wk MII oocytes at ×600 magnification. Graphical representation shows median number of sperm bound. n, number of oocytes examined from three control/MSE animals, $^{**}P < 0.0001$ Student *t*-test. **C**) Representative confocal images of MII oocytes highlighting the varying thickness of ZP (red arrows) at ×600 magnification. Graphical representation shows median zona thickness between 4-wk and 9-mo oocytes. n, number of oocytes examined from four to six control/MSE animals, $P < 0.0001$, ANOVA with Tukey post hoc. Box plot shows mean (centerline) with box outline 25th–75th percentiles and whiskers 10th–90th percentiles. Bar = 20 µm.

displayed increased rates of superoxide leakage. Oxidative stress has the potential to impact numerous aspects of oocyte maturation and development, such as meiotic spindle formation. Previous work has shown that exposure of oocytes to the pro-oxidant tertiary butyl hydroperoxide, or H_2O_2, significantly reduces spindle size in a manner similar to that observed in MSE mice [38, 52]. Correct spindle formation is critical for chromosome separation, and changes to normal MII spindle morphology in MSE oocytes could potentially lead to chromosome segregation errors during MII completion, causing aneuploidy, and ultimately embryo loss.

Furthermore, the increased lipid peroxidation in MSE oocytes, predicted to be another outcome of increased oxidative stress, may be the causative factor behind the decreased sperm-egg interactions we observed. We hypothesize that increased lipid peroxidation may have led to decreased fluidity of the oolemmal membrane, potentially altering its protein composition and impacting proteins involved in sperm-egg interaction, such as CD9 or GM1 [53, 54]. Such scenarios have been previously reported in other cell systems, including in macrophages, whereby exposure to H_2O_2 decreased plasma membrane fluidity through increasing the frequency of lipid rafts [55].

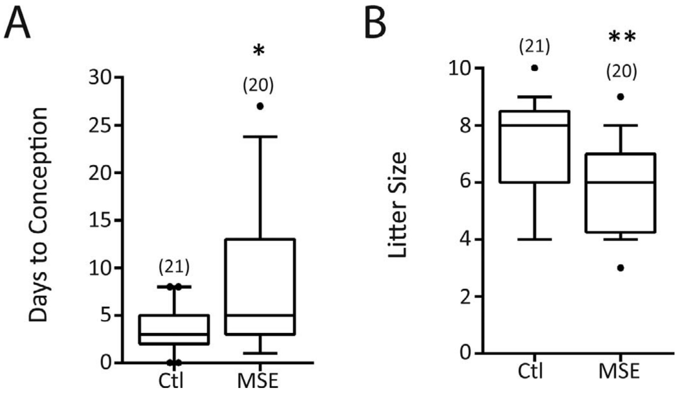

FIG. 8. Maternal smoke exposure causes reduced fertility in adult life. **A**) Average number of days to conception in control and MSE females continually housed with wild-type males (*$P = 0.0206$, Mann-Whitney test). **B**) Average litter size for control versus MSE females (*$P = 0.0190$, Student *t*-test). Results represent n = 4 control/MSE animals per group during 3 mo; box plot shows mean (centerline) with box outline 25th–75th percentiles and whiskers 10th–90th percentiles.

Sperm-zona interaction also appeared to be reduced in MSE oocytes, and interestingly these oocytes possessed a thinner ZP matrix at 4 wk. In the mouse, the ZP consists of three proteins: ZP1, ZP2, and ZP3 [56]. The importance of this structure is indicated by the fact that deletion of the ZP2 or ZP3 genes in mice causes infertility due to abnormal follicle and oocyte development [57, 58]. Although ZP1-null females display relatively normal oocyte development, similar to our observations these oocytes had a significantly thinner ZP and females had smaller litters due to embryonic loss [59]. We predict that maternal smoke exposure might influence either 1) the production of ZP components through transcriptional or translational changes, or 2) ZP glycoprotein stability or turnover. It would be of particular interest to determine whether MSE influences the expression of the ZP or other key genes involved in oocyte development, which may impact the final quality of the mature oocyte. Interestingly, however, by 9 mo zona thickness was increased in both groups. In humans a correlation between zona thickening and increasing age has been found [60]. It is therefore possible that our aging MSE mice are showing a more severe aging phenotype with respect to zona thickness such that there is negligible difference from controls by 9 mo. To support this idea, we find that MSE oocytes have a 36% increase in zona thickness with age compared with the 12% increase observed in controls.

In summary, by using a model that avoids the external confounders present in human epidemiological studies, such as lifestyle and environmental factors, we have been able to provide strong evidence that maternal smoke exposure adversely affects the reproductive health of female offspring. Our results indicate that such smoke exposure results in reduced female fertility in adult life, which can be attributed to both a reduction in the number and quality of ovulated oocytes. These findings provide an important basis for understanding the decreased fecundability and early-onset menopause observed in humans following maternal smoking. Further studies using our MSE model could be instrumental in pinpointing the effects that smoking cessation prior to conception or at different embryonic stages of pregnancy has on the fertility of the subsequent generation, and our future work will focus on the potential of transgenerational effects of MSE. Such knowledge will hopefully facilitate smoking cessation campaigns targeting young women, particularly those who are pregnant and/or breast-feeding.

ACKNOWLEDGMENT

The authors are grateful for the imaging analysis program given by Dr. Simon I.R. Lane, proofreading by Dr. Kate Redgrove, and smoke exposure performed by Kristy Wheeldon and others in the Hansbro group.

REFERENCES

1. Lee L, Lupo P. Maternal smoking during pregnancy and the risk of congenital heart defects in offspring: a systematic review and metaanalysis. Pediatr Cardiol 2013; 34:398–407.
2. Li YF, Langholz B, Salam MT, Gilliland FD. Maternal and grandmaternal smoking patterns are associated with early childhood asthma. Chest 2005; 127:1232–1241.
3. Ino T. Maternal smoking during pregnancy and offspring obesity: meta-analysis. Pediatr Int 2010; 52:94–99.
4. Hackshaw A, Rodeck C, Boniface S. Maternal smoking in pregnancy and birth defects: a systematic review based on 173 687 malformed cases and 11.7 million controls. Hum Reprod Update 2011; 17:589–604.
5. Australian Institute of Health and Welfare. National Drug Strategy Household Survey detailed report: 2013. Canberra, Australia: Australian Institute of Health and Welfare; 2014: supplementary tobacco smoking table S3.2. Drug Statistics Series No. 28. Cat. No. PHE 183.
6. Hilder L, Zhichao Z, Parker M, Jahan S, Chambers GM. Australia's mothers and babies 2012. Canberra, Australia: Australian Institute of Health and Welfare; 2014:25. Perinatal Statistics Series No. 30. Cat No. PER 69.
7. Tong VT, Dietz PM, Morrow B, D'Angelo DV, Farr SL, Rockhill KM, England LJ; Centers for Disease Control and Prevention (CDC). Trends in smoking before, during, and after pregnancy—Pregnancy Risk Assessment Monitoring System, United States, 40 sites, 2000–2010. MMWR Surveill Summ 2013; 62:1–19.
8. Ernst A, Kristensen SL, Toft G, Thulstrup AM, Håkonsen LB, Olsen SF, Ramlau-Hansen CH. Maternal smoking during pregnancy and reproductive health of daughters: a follow-up study spanning two decades. Hum Reprod 2012; 27:3593–3600.
9. Strohsnitter WC, Hatch EE, Hyer M, Troisi R, Kaufman RH, Robboy SJ, Palmer JR, Titus-Ernstoff L, Anderson D, Hoover RN, Noller KL. The association between in utero cigarette smoke exposure and age at menopause. Am J Epidemiol 2008; 167:727–733.
10. Jensen TK, Henriksen TB, Hjollund NH, Scheike T, Kolstad H, Giwercman A, Ernst E, Bonde JP, Skakkebaek NE, Olsen J. Adult and prenatal exposures to tobacco smoke as risk indicators of fertility among 430 Danish couples. Am J Epidemiol 1998; 148:992–997.
11. Jensen TK, Joffe M, Scheike T, Skytthe A, Gaist D, Petersen I, Christensen K. Early exposure to smoking and future fecundity among Danish twins. Int J Androl 2006; 29:603–613.
12. Weinberg CR, Wilcox AJ, Baird DD. Reduced fecundability in women with prenatal exposure to cigarette smoking. Am J Epidemiol 1989; 129: 1072–1078.
13. Ye X, Skjaerven R, Basso O, Baird DD, Eggesbo M, Cupul Uicab LA, Haug K, Longnecker MP. In utero exposure to tobacco smoke and subsequent reduced fertility in females. Hum Reprod 2010; 25: 2901–2906.
14. Fowler PA, Childs AJ, Courant F, MacKenzie A, Rhind SM, Antignac JP, Le Bizec B, Filis P, Evans F, Flannigan S, Maheshwari A, Bhattacharya S, et al. In utero exposure to cigarette smoke dysregulates human fetal ovarian developmental signalling. Hum Reprod 2014; 29:147–189.
15. Anderson RA, McIlwain L, Coutts S, Kinnell HL, Fowler PA, Childs AJ. Activation of the aryl hydrocarbon receptor by a component of cigarette smoke reduces germ cell proliferation in the human fetal ovary. Mol Hum Reprod 2014; 20:42–48.
16. Lutterodt MC, Sørensen KP, Larsen KB, Skouby SO, Andersen CY, Byskov AG. The number of oogonia and somatic cells in the human female embryo and fetus in relation to whether or not exposed to maternal cigarette smoking. Hum Reprod 2009; 24:2558–2566.
17. Baker TG. A quantitative and cytological study of germ cells in human ovaries. Proc R Soc Lond B Biol Sci 1963; 158:417–433.
18. Jones KT, Lane SIR, Holt JE. Start and stop signals of oocyte meiotic maturation. In: Coticchio G, Albertini DF, De Santis L, eds. Oogenesis. London, UK: Springer; 2013:183–193.
19. Camlin NJ, McLaughlin EA, Holt JE. Through the smoke: use of in vivo

and in vitro cigarette smoking models to elucidate its effect on female fertility. Toxicol Appl Pharmacol 2014; 281:266–275.
20. Knight PG, Satchell L, Glister C. Intra-ovarian roles of activins and inhibins. Mol Cell Endocrinol 2012; 359:53–65.
21. Holt JE, Lane SI, Holt KT. The control of meiotic maturation in mammalian oocytes. Curr Top Dev Biol 2013; 102:207–226.
22. Jurisicova A, Taniuchi A, Li H, Shang Y, Antenos M, Detmar J, Xu J, Matikainen T, Benito Hernández A, Nunez G, Casper RF. Maternal exposure to polycyclic aromatic hydrocarbons diminishes murine ovarian reserve via induction of Harakiri. J Clin Invest 2007; 117:3971–3978.
23. Kilic S, Yuksel B, Lortlar N, Sertyel S, Aksu T, Batioglu S. Environmental tobacco smoke exposure during intrauterine period promotes granulosa cell apoptosis: a prospective, randomized study. J Matern Fetal Neonatal Med 2012; 25:1904–1908.
24. Matikainen TM, Moriyama T, Morita Y, Perez GI, Korsmeyer SJ, Sherr DH, Tilly JL. Ligand activation of the aromatic hydrocarbon receptor transcription factor drives Bax-dependent apoptosis in developing fetal ovarian germ cells. Endocrinology 2002; 143:615–620.
25. Holloway AC, Kellenberger LD, Petrik JJ. Fetal and neonatal exposure to nicotine disrupts ovarian function and fertility in adult female rats. Endocrine 2006; 30:213–216.
26. Beckett EL, Stevens RL, Jarnicki AG, Kim RY, Hanish I, Hansbro NG, Deane A, Keely S, Horvat JC, Yang M, Oliver BG, van Rooijen N, et al. A new short-term mouse model of chronic obstructive pulmonary disease identifies a role for mast cell tryptase in pathogenesis. J Allergy Clin Immunol 2013; 131:752–762.
27. Sobinoff AP, Beckett EL, Jarnicki AG, Sutherland JM, McCluskey A, Hansbro PM, McLaughlin EA. Scrambled and fried: cigarette smoke exposure causes antral follicle destruction and oocyte dysfunction through oxidative stress. Toxicol Appl Pharmacol 2013; 271:156–167.
28. Sobinoff AP, Sutherland JM, Beckett EL, Stanger SJ, Johnson R, Jarnicki AG, McCluskey A, St John JC, Hansbro PM, McLaughlin EA. Damaging legacy: maternal cigarette smoking has long-term consequences for male offspring fertility. Hum Reprod 2014; 29:2719–2735.
29. Hansbro PM, Hamilton MJ, Fricker M, Gellatly SL, Jarnicki AG, Zheng D, Frei SM, Wong GW, Hamadi S, Zhou S, Foster PS, Krilis SA, Stevens RL. Importance of mast cell Prss31/transmembrane tryptase/tryptase-γ in lung function and experimental chronic obstructive pulmonary disease and colitis. J Biol Chem 2014; 289:18214–18227.
30. Fricker M, Deane A, Hansbro PM. Animal models of chronic obstructive pulmonary disease. Expert Opin Drug Discov 2014; 9:629–645.
31. Franklin BS, Bossaller L, De Nardo D, Ratter JM, Stutz A, Engels G, Brenker C, Nordhoff M, Mirandola SR, Al-Amoudi A, Mangan MS, Zimmer S, et al. The adaptor ASC has extracellular and 'prionoid' activities that propagate inflammation. Nat Immunol 2014; 15:727–737.
32. McCloy RA, Rogers S, Caldon CE, Lorca T, Castro A, Burgess A. Partial inhibition of Cdk1 in G2 phase overrides the SAC and decouples mitotic events. Cell Cycle 2014; 13:1400–1412.
33. Holt JE, Lane SI, Jennings P, García-Higuera I, Moreno S, Jones KT. APCFZR1 prevents non-disjunction in mouse oocytes by controlling meiotic spindle assembly timing. Mol Biol Cell 2012; 23:3970–3981.
34. Lane SIR, Jones KT. Non-canonical function of spindle assembly checkpoint proteins after APC activation reduces aneuploidy in mouse oocytes. Nat Commun 2014; 5:3444.
35. Jennings PC, Merriman JA, Beckett EL, Hansbro PM, Jones KT. Increased zona pellucida thickness and meiotic spindle disruption in oocytes from cigarette smoking mice. Hum Reprod 2011; 26:878–884.
36. Oktay K, Schenken RS, Nelson JF. Proliferating cell nuclear antigen marks the initiation of follicular growth in the rat. Biol Reprod 1995; 53: 295–301.
37. Durlinger ALL, Gruijters MJ, Kramer P, Karels B, Kumar TR, Matzuk MM, Rose UM, de Jong FH, Uilenbroek JT, Grootegoed JA, Themmen AP. Anti-Müllerian hormone attenuates the effects of FSH on follicle development in the mouse ovary. Endocrinology 2001; 142:4891–4899.
38. Tarín JJ, Vendrell FJ, Ten J, Blanes R, van Blerkom J, Cano A. The oxidizing agent tertiary butyl hydroperoxide induces disturbances in spindle organization, c-meiosis, and aneuploidy in mouse oocytes. Mol Hum Reprod 1996; 2:895–901.
39. Sobinoff AP, Mahony M, Nixon B, Roman SD, McLaughlin EA. Understanding the Villain: DMBA-induced preantral ovotoxicity involves selective follicular destruction and primordial follicle activation through PI3K/Akt and mTOR signaling. Toxicol Sci 2011; 123:563–575.
40. Sobinoff AP, Nixon B, Roman SD, McLaughlin EA. Staying alive: PI3K pathway promotes primordial follicle activation and survival in response to 3MC-induced ovotoxicity. Toxicol Sci 2012; 128:258–271.
41. Sobinoff AP, Pye V, Nixon B, Roman SD, McLaughlin EA. Jumping the gun: smoking constituent BaP causes premature primordial follicle activation and impairs oocyte fusibility through oxidative stress. Toxicol Appl Pharmacol 2012; 260:70–80.
42. Essers J, Theil AF, Baldeyron C, van Cappellen WA, Houtsmuller AB, Kanaar R, Vermeulen W. Nuclear dynamics of PCNA in DNA replication and repair. Mol Cell Biol 2005; 25:9350–9359.
43. Kim MR, Tilly JL. Current concepts in Bcl-2 family member regulation of female germ cell development and survival. Biochim Biophys Acta 2004; 1644:205–210.
44. McLaughlin EA, McIver SC. Awakening the oocyte: controlling primordial follicle development. Reproduction 2009; 137:1–11.
45. Yu FQ, Han CS, Yang W, Jin X, Hu ZY, Liu YX. Role of ERK1/2 in FSH induced PCNA expression and steroidogenesis in granulosa cells. Front Biosci 2005; 10:896–904.
46. El-Hefnawy T, Zeleznik AJ. Synergism between FSH and activin in the regulation of proliferating cell nuclear antigen (PCNA) and cyclin D2 expression in rat granulosa cells. Endocrinology 2001; 142:4357–4362.
47. Nair S, Slaughter JC, Terry JG, Appiah D, Ebong I, Wang E, Siscovick DS, Sternfeld B, Schreiner PJ, Lewis CE, Kabagambe EK, Wellons MF. Anti-mullerian hormone (AMH) is associated with natural menopause in a population-based sample: the CARDIA Women's Study. Maturitas 2015; 81:493–498.
48. Shaw ND, Srouji SS, Welt CK, Cox KH, Fox JH, Adams JA, Sluss PM, Hall JE. Compensatory increase in ovarian aromatase in older regularly cycling women. J Clin Endocrinol Metab 2015; 100:3536–3547.
49. Gulhan I, Bozkaya G, Uyar I, Oztekin D, Pamuk BO, Dogan E. Serum lipid levels in women with premature ovarian failure. Menopause 2012; 19:1231–1234.
50. Knauff EA, Westerveld HE, Goverde AJ, Eijkemans MJ, Valkenburg O, van Santbrink EJ, Fauser BC, van der Schouw YT. Lipid profile of women with premature ovarian failure. Menopause 2008; 15:919–923.
51. Albrecht ED, Pepe GJ. Estrogen regulation of placental angiogenesis and fetal ovarian development during primate pregnancy. Int J Dev Biol 2010; 54:397–408.
52. Zhang X, Wu XQ, Lu S, Guo YL, Ma X. Deficit of mitochondria-derived ATP during oxidative stress impairs mouse MII oocyte spindles. Cell Res 2006; 16:841–850.
53. Żyłkiewicz E, Nowakowska J, Maleszewski M. Decrease in CD9 content and reorganization of microvilli may contribute to the oolemma block to sperm penetration during fertilization of mouse oocyte. Zygote 2010; 18: 195–201.
54. Van Blerkom J, Caltrider K. Sperm attachment and penetration competence in the human oocyte: a possible aetiology of fertilization failure involving the organization of oolemmal lipid raft microdomains influenced by the $\Delta\Psi$m of subplasmalemmal mitochondria. Reprod Biomed Online 2013; 27:690–701.
55. de la Haba C, Palacio JR, Martínez P, Morros A. Effect of oxidative stress on plasma membrane fluidity of THP-1 induced macrophages. Biochim Biophys Acta 2013; 1828:357–364.
56. Wassarman PM, Litscjer ES. Influence of the zona pellucida of the mouse egg on folliculogenesis and fertility. Int J Dev Biol 2012; 56:833–839.
57. Rankin TL, O'Brien M, Lee E, Wigglesworth K, Eppig J, Dean J. Defective zonae pellucidae in Zp2-null mice disrupt folliculogenesis, fertility and development. Development 2001; 128:1119–1126.
58. Liu C, Litscher ES, Mortillo S, Sakai Y, Kinloch RA, Stewart CL, Wassarman PM. Targeted disruption of the mZP3 gene results in production of eggs lacking a zona pellucida and infertility in female. Proc Natl Acad Sci U S A 1996; 93:5431–5436.
59. Rankin T, Talbot P, Lee E, Dean J. Abnormal zonae pellucidae in mice lacking ZP1 result in early embryonic loss. Development 1999; 126: 3847–3855.
60. Nawroth F, Müller P, Wolf C, Sudik R. Is the zona pellucida thickness of metaphase-II oocytes in an IVF/ICSI program influenced by the patient's age? Gynecol Obstet Invest 2001; 52:55–59.